Contrib Mineral Petrol (2005) 149: 446–461
DOI 10.1007/s00410-005-0658-7

ORIGINAL PAPER

Anthi Liati · Nikolaus Froitzheim · C. Mark Fanning

Jurassic ophiolites within the Valais domain of the Western and Central Alps: geochronological evidence for re-rifting of oceanic crust

Received: 2 August 2004 / Accepted: 9 February 2005 / Published online: 13 April 2005

Abstract Metabasic rocks from different parts of the Antrona ophiolites, Western Alps, as well as from the Misox zone, Central Alps, were dated using ion microprobe (SHRIMP) U-Pb analyses of zircon, in association with cathodoluminescence (CL) imaging. HP metamorphism must have affected at least the major part of the Antrona ophiolites, although HP relics are rarely preserved, probably due to the Lepontine metamorphic overprint. HP metamorphism has affected also the area of the Misox zone. The origin of the Antrona ophiolites is arguable. They were interpreted as part of both the Piemont–Ligurian (PL) and the Valais ocean, the two main oceans in the area of the Alps before Alpine convergence. SHRIMP-analyses of co-magmatic zircon domains from the Antrona ophiolites (Guggilihorn, Passo del Mottone and Quarata areas) yielded identical (within uncertainty) weighted mean $^{206}Pb/^{238}U$ ages of 155.2 ± 1.6 Ma, 158 ± 17 Ma (or 163.1 ± 2.4 Ma: one analysis; 1σ error) and 155.6 ± 2.1 Ma, respectively, interpreted as the time of crystallization of the magmatic protoliths. These Late Jurassic ages fit well to the time span considered for the formation of Piemont–Ligurian oceanic crust. The metagabbro of the Misox zone (Hinterrhein area), for which a Valaisan origin is generally accepted, gave also a Late Jurassic, PL protolith age of 161.0 ± 3.9 Ma. The metamorphic zircon domains from the amphibolitized eclogite of Mottone yielded an age of 38.5 ± 0.7 Ma, interpreted as the time of HP metamorphism. This age is in good agreement with the time of metamorphism reported from previous zircon SHRIMP-data for eclogites and amphibolites of other parts in the Valais domain. In order to bring in line the PL protolith ages with the Valaisan metamorphic ages, we suggest a scenario involving emplacement of part of the PL oceanic crust to the north of the newly formed Briançonnais peninsula, inside the Valais geotectonic domain. This paleotectonic configuration was probably established when younger Valaisan oceanic crust formed by spreading and re-rifting, partly within PL oceanic crust.

Communicated by W. Schreyer

A. Liati (✉)
Institute of Isotope Geology and Mineral Resources,
Swiss Federal Institute of Technology (ETH),
Sonneggstrasse 5, 8092 Zurich, Switzerland
E-mail: liati@erdw.ethz.ch

N. Froitzheim
Geological Institute, University of Bonn,
Nussallee 8, 53115 Bonn, Germany

C. M. Fanning
Research School of Earth Sciences,
The Australian National University, Mills Road,
Canberra, 0200 Australia

Introduction

The Alpine chain formed as a result of subduction/collision and exhumation of continental and oceanic fragments between the European and Adriatic plates. A series of still not well-understood tectono-metamorphic processes associated with subduction, collision and exhumation of the different rock sequences in the Alps resulted in highly complex nappe structures. Reliable geochronological data from metabasic rocks, which constitute part of the different geotectonic units of the Alps, have the potential to provide important information and thus contribute to a better understanding of the paleogeography and geodynamic evolution of the Alpine orogen.

Metabasic rocks in the Alps commonly represent remnants of the Piemont–Ligurian (PL) ocean, also known as South Penninic, and the Valais ocean, known as North Penninic ocean. The PL ocean, which represents the Mesozoic Tethys, was the main oceanic basin and opened from the Middle Jurassic onward (e.g. De Wever and Baumgartner 1995). The Valais ocean was a smaller basin opening from the Late

Jurassic–Early Cretaceous onward (e.g., Frisch 1979; Trümpy 1980; Florineth and Froitzheim 1994; Stampfli et al. 1998). It was separated from the PL ocean by the Briançonnais peninsula, which thinned to the east so that only one Penninic ocean existed in the eastern part of the Alps (e.g. Trümpi 1980; Oberhänsli 1994; Schmid et al. 1996). Different models were proposed for the paleogeographic configuration and extent in space and time of these two oceans in the Alps, prior to the onset of the Alpine orogeny (e.g. review by Escher et al. 1997; Froitzheim 2001 and references therein).

Within the framework of the present paper, we have dated metabasic rocks from different parts of the Antrona ophiolites, Western Alps, as well as from the Misox zone, Central Alps (Fig. 1). For the Misox zone, there is a consensus that it is part of the Valais ocean, while different opinions exist about the Antrona ophiolites (see below). We have dated rocks from the above domains in order to constrain the extent, the palaeogeographic relationships and the geodynamic evolution of these two oceans. Because of the complex geological evolution of the dated rocks, which involves a magmatic pre-history and metamorphic overprint(s), we have used the U-Pb zircon ion microprobe dating method (SHRIMP) of the mineral zircon. SHRIMP-dating was assisted by cathodoluminescence (CL) imaging of the zircon crystals, enabling us to examine the internal structure of the sectioned zircon crystals and to select suitable analysis areas that characterise single periods of growth.

Geological framework

Antrona ophiolites—Western Alps

The Antrona ophiolites occur as a narrow, complexly folded zone between three continental gneiss units: the Monte Rosa nappe, the Camughera–Moncucco unit, and the St. Bernard nappe system, which belongs to the Briançonnais domain (Figs. 1, 2a). They consist of amphibolites (partly with eclogite relics, mainly in the western part) and serpentinites, while marbles and calcschists constitute the former sedimentary cover. A series of hypotheses based on structural grounds were formulated about the paleogeographic origin of the Antrona ophiolites and the Monte Rosa nappe (Fig. 3). According to Escher et al. (1997), the Antrona ophiolites are interpreted as part of the Zermatt-Saas ophiolites (PL ocean), in which case the Monte Rosa nappe constitutes part of the Briançonnais microcontinent. Alternatively, it was proposed that the Antrona ophiolites are part of the Valais basin (Froitzheim 2001; Keller and Schmid 2001) and the Monte Rosa nappe is part of the European margin (Froitzheim 2001). This view was also suggested on the basis of SHRIMP data (Rubatto and Gebauer 1999; Liati and Gebauer 2001, see also below). An origin of the Antrona ophiolites from an independent oceanic basin (e.g., Platt 1986) was also suggested. In this case, the Monte Rosa nappe would represent an additional microcontinent.

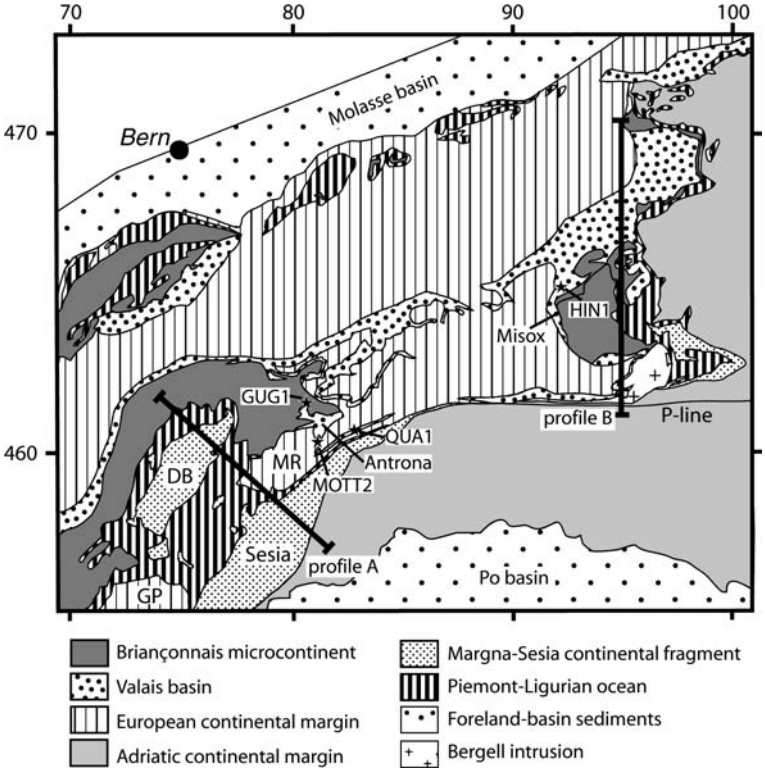

Fig. 1 Tectonic map of the Swiss–Italian Alps showing the location of the Antrona ophiolites and of the Misox zone, as well as the sample localities. For profiles **a** and **b**, see Fig. 2 . *GP* Gran Paradiso; *DB* Dent Blanche; *MR* Monte Rosa; P-line: Periadriatic line. GUG1, MOTT2, QUA1 and HIN1: samples dated (see text)

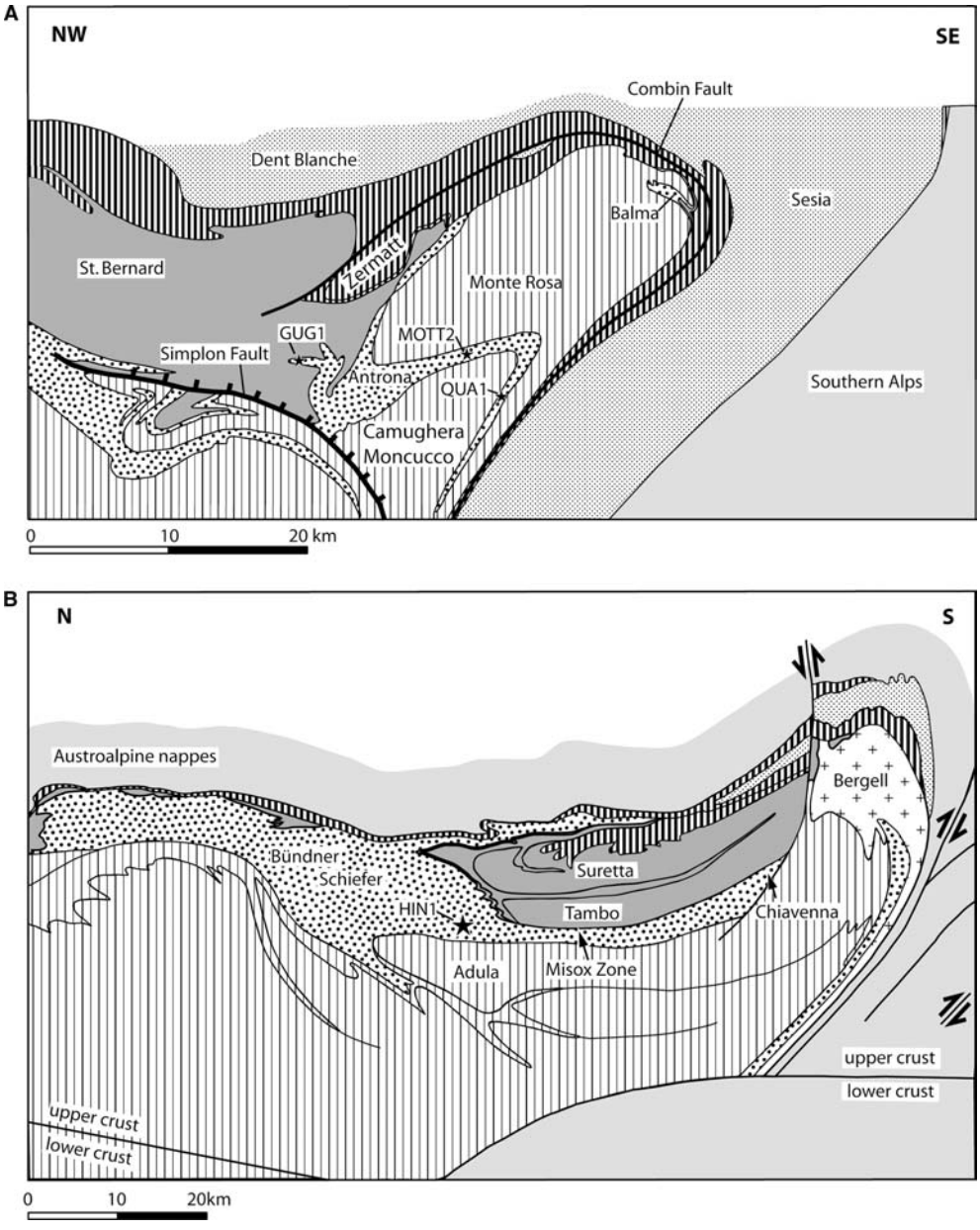

Fig. 2 Tectonic profiles **a** and **b** through the Alps showing also the sample locations (GUG1, MOTT2, QUA1 and HIN1). **a** Western Alps: the tectonic position of the Antrona ophiolites and their relationship to the surrounding units is shown. Modified after Escher et al. (1997) and Froitzheim (2001). Balma unit (Valaisan on the southern side of Monte Rosa; see also Liati et al. 2002). **b** Central Alps: the position of the Misox zone and its relationship to the surrounding units is given (after Schmid et al. 1996). Location of both profiles is given in Fig. 1. Patterns as in Fig. 1

Metamorphic rocks in the Antrona ophiolites predominantly record PT conditions of the greenschist-facies and amphibolite-facies, probably as a result of the Tertiary (Lepontine) metamorphism (see e.g. Colombi 1989; Pfeiffer et al. 1989). It is noted here that the term "Lepontine" was introduced to describe the high-grade Tertiary metamorphism of rocks in the area between the Gotthard massif in the north and the Insubric line in the south, and between the Simplon area in the west and the Bergell area in the east (e.g., Wenk 1956; Trommsdorff 1966; Frey and Ferreiro-Mählmann 1999 and references therein). The Lepontine metamorphism was considered to have taken place at ca. 38 Ma (Jäger 1973), in both the southern European margin and the Briançonnais terrane. Recent geochronological studies revealed, however, a temperature peak at ca. 33 Ma for the Lepontine metamorphism in units belonging to the southern European margin (see summary by Gebauer 1999). For the Antrona ophiolites, an increase in metamorphic grade from greenschist- to upper amphibolite-facies conditions, from the northwestern to the southeastern and eastern part was suggested (see Colombi 1989 or Pfeiffer et al. 1989 for details on this issue). Eclogite-facies relics of an earlier metamorphic stage (or possibly of an earlier metamorphic cycle) occur in the metabasic rocks of the western part. It is unclear, however, whether all of the Antrona ophiolites have suffered eclogite-facies metamorphism or not. It is well possible that eclogite-facies relics were entirely obliterated in the eastern part, where the rocks were overprinted under higher temperature conditions during the Lepontine stage.

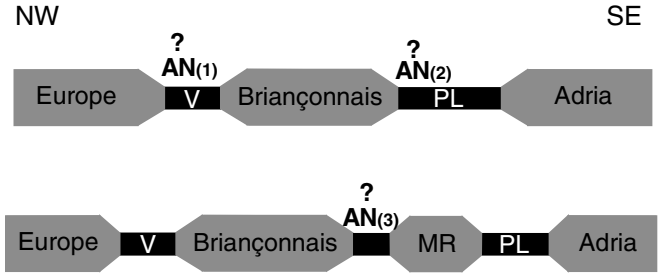

Fig. 3 Schematic illustration of the different hypotheses suggested for the paleogeographic location of origin of the Antrona ophiolites: (1): Froitzheim (2001); Keller and Schmid (2001); (2): Escher et al. (1997); (3): Platt (1986). *AN* Antrona; *V* Valais; *PL* Piemont-Ligurian; *MR* Monte Rosa

Misox zone—Central Alps

The Misox zone, between the Adula nappe (below) to the west and the Tambo nappe (above) to the east, includes rock sequences of the 'Bündnerschiefer' (Figs. 1, 2b) and is generally regarded to be part of the Valais basin (e.g., Schmid et al. 1996). It consists of calc-schists, as well as greenschists, metagabbros, and lenses of gneiss (e.g. Gansser 1937). Its thickest parts reach ca. 800 m and, as it thins to the south, close to Passo della Forcola, the Adula nappe comes into direct contact with the Tambo nappe. The Misox zone is subdivided, from base to top, into the "Adulatrias" (Gansser 1937) which is in fact a mélange zone (Pescion zone; Pleuger et al. 2003), the Lower Uccello zone (typical Bündnerschiefer with greenschist layers and metagabbro, including our sample locality), the Gadriolzug (paragneiss, orthogneiss, and marble), the Upper Uccello zone (mainly Bündnerschiefer), and higher slivers mainly derived from the Briançonnais realm. In the Misox zone and the 'Vals Bündnerschiefer' farther north, high-P metamorphism ($P > 12$ kbar, $T = 460$–560°C) with blue amphibole was reported (e.g., Heinrich 1983; Oberhänsli 1986; Ring 1992).

Sample description

Antrona ophiolites—Western Alps

We collected samples for dating from three different areas of the Antrona ophiolites: at Guggilihorn (SE of Simplon), at Passo del Mottone and at Quarata, south of Domodossola (Figs. 1, 2a).

(a) Guggilihorn, SE of Simplon (Figs. 1, 2a, sample GUG1): the dated rock is a metagabbro metamorphosed and deformed under greenschist-facies to amphibolite-facies conditions. A flaser-gabbro structure is still visible. This metagabbro is associated with other rock types of the Antrona ophiolite series, such as calcschists, serpentinites, and other metabasic rocks, presumably metabasalts. The common mineral assemblage is: epidote, plagioclase, amphibole, chlorite, white mica, quartz, titanite, zircon and opaque phases. Eclogite-facies mineral relics or textural evidence of a preceding HP metamorphism are not reported and were also not found in the mineral assemblage of the dated rock. However, our detailed study of micro-inclusions within the zircon crystals has revealed the presence of phengite inclusions within metamorphic zircon domains. As is described below (Sect. 5.1), the Si content of these phengites points to minimum P conditions of ca. 13–15 kbar (for an assumed T range of 500–650°C). It seems, therefore, that the upper greenschist- to amphibolite-facies assemblage of the dated metagabbro is the result of strong retrogression, post-dating an earlier HP metamorphism. Eclogite-facies metamorphism is identified in other areas of the narrow zone of the Antrona ophiolites, south of Guggilihorn (Fig. 1; e.g., Colombi and Pfeiffer 1986). It is also noted that in the Explanatory Notes of the Tectonic map of Western Switzerland, the area of Guggilihorn, where the dated metagabbro occurs, is included in the broad area of Antrona ophiolites characterized by eclogite-facies metamorphism (Steck et al. 2001).

(b) Passo del Mottone (Figs. 1, 2a, sample MOTT2): Two amphibolitized eclogites were collected from this area. Only one of them contained zircons. The mineral assemblage of this rock is: garnet, hornblende, epidote, quartz, plagioclase, rutile, sphene ± calcite, zircon and opaque phases. Omphacite relics or symplectites of clinopyroxene + albite, commonly described for metabasic rocks of this area (e.g., Colombi and Pfeiffer, 1986) were not observed in this particular rock, obviously because it was affected by a more complete amphibolite-facies equilibration. Metamorphic conditions of $P > 14$–16 kbar, $T = 500$–700°C were reported for the eclogite-facies metamorphism in this area (Colombi and Pfeiffer 1986).

(c) Quarata, S' of Domodossola (Figs. 1 and 2a, sample QUA1): The dated rock is an amphibolite with the common mineral assemblage: green hornblende, plagioclase, epidote, titanite (some with rutile inclusions) and quartz. Colombi (1989) reports PT conditions of the medium to upper amphibolite-facies for metabasic rocks of this area. No HP relics are reported. However, it is worth mentioning that in the amphibolite dated, as well as in other amphibolite samples collected from this area within the framework of the present study, rutile relics were observed within titanite. According to empirical observations and experimental data (e.g. Hellman and Green 1979), rutile is commonly the Ti-phase in high-pressure metabasites, although it may be present also in amphibolites that have not suffered high-pressure metamorphism. Although not conclusive, the presence of rutile in the amphibolites of Quarata suggests that they may have been subjected to metamorphic conditions of higher pressure than indicated by their current mineralogical composition.

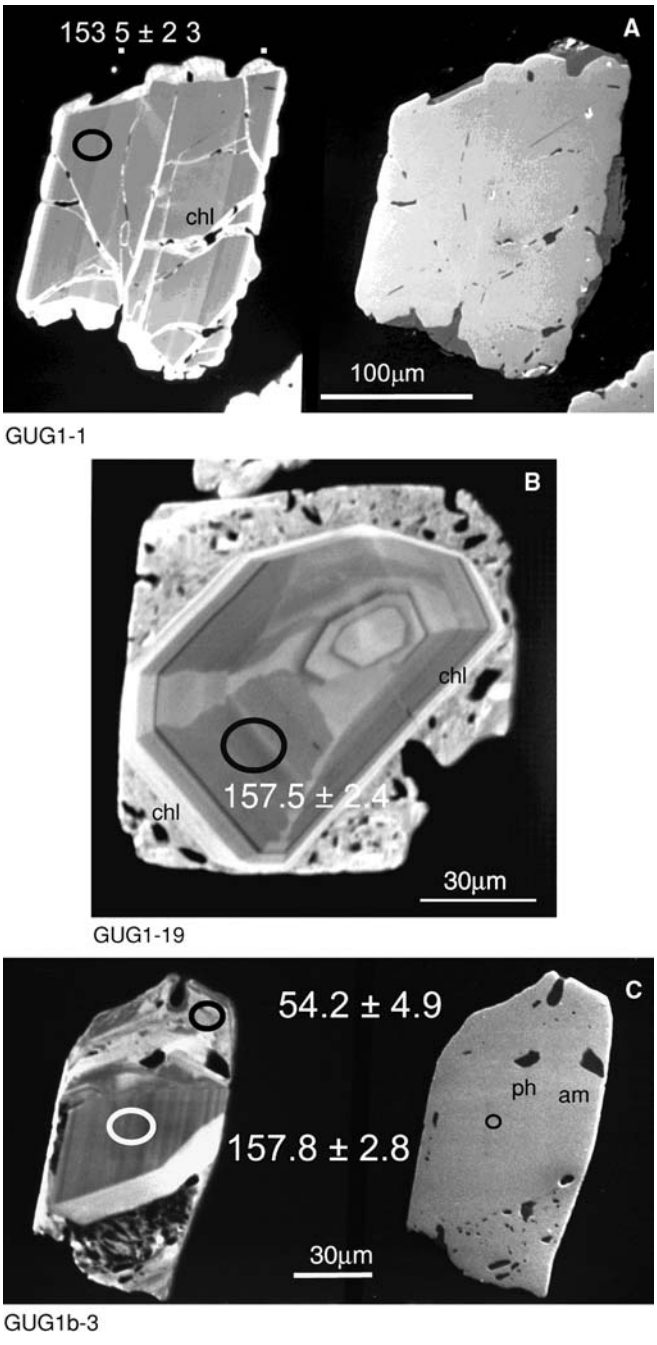

Fig. 4 Cathodoluminescence (CL; left part of **a**, **c** and the whole of picture **b**) and secondary electron (SE) images (*right part* of **a** and **c**) of zircon crystals from the metagabbro of Guggilihorn, Antrona ophiolites. Note the bright CL domains along cracks crosscutting the magmatic zircon domain of (**a**), visible only on the CL. These bright CL domains probably formed by fluid circulation along cracks (later healed), during post-crystallization (metamorphic) event(s). An oscillatory zoned domain (of magmatic origin) surrounded by a metamorphic rim bright in CL (in **a**) or with abundant ''inclusions'' in (**b**) and (**c**) are shown. The ''inclusions'' were trapped inside the zircons during their growth and most of them were later altered due to the action of fluids along cracks (see text for details). Representative electron microprobe analyses of such inclusions are given in Table 1. The ages given apply to the *areas circled*. *chl* chlorite; *am* amphibole; *ph* phengite

It is worth noting that the zircons sectioned from this rock do not show any metamorphic rims (see also below, under Sect. 5.3). Based on CL studies of numerous metamorphic zircons from many orogens worldwide, development of metamorphic rims is observed in zircons from rocks that were subjected to metamorphic T at or above ca. 650°C, unless abundant fluids were present (see e.g., Vavra et al. 1999 or Liati and Gebauer 2003 and references therein for this issue). An abundance of fluids may contribute significantly to the development of metamorphic rims at lower T. The absence of metamorphic rims in zircons from the Quarata amphibolite suggests, therefore, that this rock was probably affected by metamorphic temperatures lower than ca. 650°C (compare also with Sect. 3.2 below).

Misox zone (Hinterrhein)—Central Alps

The dated rock is a metabasite from the area of Hinterrhein (Figs. 1, 2a, sample HIN1), belonging to the ophiolites of the Lower Uccello zone (Gansser 1937) and bearing the common mineral assemblage: clinozoisite, plagioclase, actinolite/tremolite, chlorite, talc, quartz and sphene. No critical HP minerals were observed in this rock. However, HP mineral relics, such as omphacite and blue amphibole were described in metabasic rocks nearby (Heinrich 1983; Oberhänsli 1986; Ring 1992), thus implying an earlier stage of HP metamorphism ($P > 12$ kbar, $T = 460$–560°C; Ring 1992). Equilibration conditions of $P = 5$–6 kbar, at T ca. 450°C are reported for the post-HP, overprinting metamorphic stage (Ring 1992). HP metamorphic relics are also described in metasediments of this area (Heinrich 1983, Chap. 3.7, p74).

The zircons from the metabasic rock of Hinterrhein do not show any metamorphic rims, similar to those from the Quarata amphibolite (Sect. 3.1). This is in agreement with the low temperatures also experienced by this rock, as development of metamorphic rims in zircon generally requires higher T (ca. >650°C; see above under Sect. 3.1).

Analytical techniques

SHRIMP-dating, CL-imaging and data evaluation

The data listed in Table 2 were obtained on SHRIMP II at The Australian National University in Canberra (sample GUG1 and most analyses of sample MOTT2), as well as on SHRIMP II at the Geological Survey of Canada in Ottawa (samples QUA1 and HIN1). The spot size used was typically around 20 µm. In exceptional cases, where the analyzed zircon domains were very narrow, a 10 µm spot was used. For data collection, seven scans were made through the mass spectrum. For a detailed description on the SHRIMP technique, data

Table 1 Electron microprobe analyses of micro-inclusions within metamorphic zircon domains of the metagabbro at Guggilihorn

	Phengite		Chlorite		Amphibole	
	GUG1B-3-2	GUG1B-3-3	GUG1B-1-1	GUG1-16-3	GUG1-16-1	GUG1B-3-1
SiO_2	52.9	53.7	29.2	27.8	57.2	56.3
TiO_2	0.27	0.22	0.03	0.04	0.01	0.03
Al_2O_3	25.2	27.1	19.5	22.0	1.59	3.68
Cr_2O_3	0.04	0.07	0.30	0.32	0.02	0.11
FeO	1.65	1.61	10.8	12.1	5.96	7.16
MnO	0.03	0.02	0.17	0.11	0.21	0.16
MgO	6.03	4.53	25.5	23.6	20.0	18.8
CaO	0.83	0.19	0.00	0.03	12.5	11.1
Na_2O	0.32	0.25	0.02	0.02	0.21	0.77
K_2O	9.60	9.41	0.02	0.06	0.08	0.08
Total	96.87	97.12	85.54	86.08	97.78	98.19
Structural formula on the basis of:						
	11 [O]		28 [O]		23 [O]	
Si	3.454	3.472	5.819	5.544	7.930	7.790
Al^{iv}	0.546	0.528	2.181	2.456	0.070	0.210
Sum	4.000	4.000	8.000	8.000	8.000	8.000
Al^{vi}	1.393	1.535	2.399	2.714	0.190	0.390
Ti	0.013	0.011	0.004	0.006	0.001	0.003
Cr	0.002	0.003	0.071	0.076	0.002	0.012
Fe	0.090	0.087	1.800	1.921	0.692	0.829
Mn	0.002	0.001	0.029	0.019	0.025	0.019
Mg	0.587	0.436	7.576	7.016	4.127	3.880
Ca	0.058	0.013	0.000	0.006	1.858	1.649
Na	0.041	0.031	0.008	0.008	0.055	0.208
K	0.800	0.776	0.005	0.015	0.015	0.013

processing including the reasons for using mainly $^{206}Pb/^{238}U$-ages for Phanerozoic zircons the reader is referred to Compston et al. (1992) and Williams (1998) or Stern (1997).

CL images of the zircon crystals were obtained both before SHRIMP-dating, to distinguish between different zircon domains, as well as after SHRIMP-dating to confirm the exact location of the spots. The CL pictures of zircon crystals were produced at the ETH in Zurich, on a CamScan CS 4 scanning electron microscope (SEM) operating at 13 kV (see Gebauer 1996 for detailed technical description). The SEM is equipped with an ellipsoidal mirror that is located close to the sample within the vacuum chamber. The sample can be located in one focal point while the second focal point lies outside the sample chamber. Here, the CL-light enters a highly sensitive photo multiplier through a quartz glass–vacuum window and a light channel. The signal of the photo multiplier is then used to produce the CL-image via a video-amplifier. Secondary electron (SE)-pictures were produced on the same CamScan CS 4 scanning electron microscope, simultaneously with the CL-pictures using a different detector.

For the calculation of the $^{238}U/^{206}Pb$ ratios and ages, the data were corrected for common Pb using the ^{207}Pb correction method. In this paper, the data are graphically presented on Tera–Wasserburg (TW) diagrams (Tera and Wasserburg 1972), where total $^{207}Pb/^{206}Pb$ versus the calibrated, total $^{238}U/^{206}Pb$ are plotted. This diagram enables one to readily assess the amount of common Pb of the individual analyses plotted. The amount of common Pb was calculated using the isotope composition of common Pb obtained from the model of Cumming and Richards (1975). The ellipses of the individual data points on the TW diagrams are plotted with a 2σ error.

For the samples measured at ANU, the U/Pb ratios were calibrated relative to AS3 and FC1 reference zircons (Paces and Miller 1993), while U and Th concentrations were calculated relative to SL13 (e.g. Compston et al. 1992; Williams 1998). For the samples analyzed at GSC, U/Pb ratios were calibrated relative to standard BR266, which is a piece of a Sri Lankan gem-quality zircon (Stern and Amelin 2003).

For the individual analyses listed in Table 2 or shown on the zircon pictures, 1σ errors are given. Finally, the ages were calculated as weighted mean ages and the error at the 95% confidence level (c.l.), taking into consideration the 1σ analytical error shown in Table 2. All diagrams and weighted mean ages were calculated with the ISOPLOT program of Ludwig (2000).

Electron microprobe analyses

Mineral inclusions in metamorphic domains of the zircon crystals were analyzed by electron microprobe. Microprobe analyses were carried out with a Cameca SX51 (at 15 kV, 20 nA) at the Institute of Mineralogy,

Table 2 U, Th, Pb SHRIMP data for co-magmatic and metamorphic zircons from metabasic rocks of the Western Alps (Antrona ophiolites: areas of Guggilihorn, Passo del Mottone and Quarata) and of the Central Alps (Misox zone: area of Hinterrhein)

	Sample	U (ppm)	Th (ppm)	Th/U	rad.Pb (ppm)	f_{206}	$^{238}U/^{206}Pb$ (1σ) (uncorrected)	$^{207}Pb/^{206}Pb$(1σ) (uncorrected)	$^{206}Pb/^{238}U$ (radiogenic)	Age (Ma) (1σ) $^{206}Pb/^{238}U$
Antrona ophiolites–Western Alps										
Metagabbro of Guggilihorn										
co-magmatic domains										
1.	GUG1-1.1	137	76	0.55	2.9	0.54	41.27 ± 0.61	0.0534 ± 0.0016	0.0241 ± 0.0004	153.5 ± 2.3
2.	GUG1-4.1	165	57	0.34	3.5	0.08	41.03 ± 0.61	0.0498 ± 0.0016	0.0243 ± 0.0004	155.1 ± 2.3
3.	GUG1-13.1	107	48	0.44	2.4	0.02	38.74 ± 0.64	0.0696 ± 0.0026	0.0252 ± 0.0004	160.2 ± 2.7
4.	GUG1-13.2	956	1011	0.67	19.9	0.19	41.21 ± 0.46	0.0506 ± 0.0007	0.0242 ± 0.0003	154.3 ± 1.7
5.	GUG1-13.3	135	69	0.51	2.8	0.18	41.95 ± 0.64	0.0505 ± 0.0017	0.0238 ± 0.0004	151.6 ± 2.3
6.	GUG1-19.1	149	69	0.46	3.2	0.27	40.32 ± 0.63	0.0513 ± 0.0017	0.0247 ± 0.0004	157.5 ± 2.4
7.	GUG1-23.1	12	8	0.67	0.3	0.11	36.01 ± 1.40	0.1377 ± 0.0100	0.0247 ± 0.0011	157.2 ± 6.9
8.	GUG1b-3.1	93	52	0.56	2.0	0.01	39.86 ± 0.70	0.0590 ± 0.0022	0.0248 ± 0.0004	157.8 ± 2.8
9.	GUG1b-4.2	49	22	0.45	1.0	0.84	42.01 ± 0.94	0.0558 ± 0.0039	0.0236 ± 0.0005	150.4 ± 3.4
10.	GUG1b-6.1	127	64	0.50	2.7	0.74	40.24 ± 0.65	0.0551 ± 0.0019	0.0247 ± 0.0004	157.1 ± 2.5
11.	*GUG1-13.5*	*32*	*14*	*0.45*	*0.8*	*0.23*	*33.80 ± 1.31*	*0.2299 ± 0.0401*	*0.0229 ± 0.0019*	*145.7 ± 12.2*
12.	*GUG1-2.1*	*15*	*8*	*0.55*	*0.3*	*0.06*	*42.44 ± 1.62*	*0.1004 ± 0.0076*	*0.0220 ± 0.0009*	*140.5 ± 5.7*
13.	*GUG1-13.4*	*20*	*10*	*0.50*	*0.4*	*0.16*	*43.44 ± 1.78*	*0.1741 ± 0.0167*	*0.0194 ± 0.0010*	*123.8 ± 6.6*
										WM: 155.2 ± 1.6 Ma
Metamorphic domains										
15.	GUG1b-7.1	86	7	0.08	0.9	0.06	80.48 ± 4.64	0.0929 ± 0.0067	0.0117 ± 0.0007	75.1 ± 4.4
16.	GUG1-28.1	80	1	0.02	0.8	0.09	84.59 ± 2.30	0.1241 ± 0.0091	0.0107 ± 0.0004	68.5 ± 2.2
17.	GUG1b-1.1	72	3	0.04	0.7	0.11	93.83 ± 2.71	0.1322 ± 0.0099	0.0095 ± 0.0003	61.0 ± 2.2
18.	GUG1b-4.1	10	0	0.02	0.1	0.25	88.08 ± 5.24	0.2505 ± 0.0318	0.0084 ± 0.0008	54.2 ± 4.9
Eclogite of Mottone										
co-magmatic domains										
19.	MOTT2-9.1	886	452	0.51	24	0.00	39.06 ± 0.58	0.0484 ± 0.0006	0.0256 ± 0.0004	163.1 ± 2.4
20.	012/MOTT2-3.1	1163	460	0.41	29	0.29	41.43 ± 0.89	0.0514 ± 0.0004	0.0241 ± 0.0001	153.3 ± 3.3
21.	012/MOTT2-10.1	3229	3403	1.09	95	0.18	42.14 ± 1.02	0.05049 ± 0.0012	0.0237 ± 0.0006	150.9 ± 3.6
22.	*MOTT2-8.1*	*985*	*657*	*0.67*	*25*	*0.16*	*43.43 ± 0.74*	*0.0503 ± 0.0008*	*0.0230 ± 0.0004*	*146.5 ± 2.5*
23.	*MOTT2-2.1*	*529*	*333*	*0.63*	*12*	*0.00*	*46.50 ± 0.61*	*0.0488 ± 0.0008*	*0.0215 ± 0.0003*	*137.2 ± 1.8*
24.	*MOTT2-4.1*	*490*	*383*	*0.78*	*12*	*0.00*	*47.33 ± 0.64*	*0.0486 ± 0.0007*	*0.0211 ± 0.0003*	*134.8 ± 1.8*
25.	*MOTT2-9.2*	*257*	*132*	*0.52*	*5*	*0.00*	*49.39 ± 1.53*	*0.0482 ± 0.0014*	*0.0203 ± 0.0006*	*129.3 ± 4.0*
26.	*MOTT2-9.3*	*327*	*192*	*0.59*	*7*	*0.21*	*49.22 ± 0.67*	*0.0503 ± 0.0007*	*0.0203 ± 0.0003*	*129.4 ± 1.7*
										WM: 158 ± 17
Metamorphic domains										
27.	002/MOTT2-B2.1	278	3	0.01	1	0.09	163.39 ± 3.31	0.0713 ± 0.0034	0.0059 ± 0.0001	38.1 ± 0.8
28.	003/MOTT2-20.1	277	2	0.01	1	0.20	167.4 ± 3.47	0.0688 ± 0.0049	0.0058 ± 0.0001	37.3 ± 0.8
29.	003/MOTT2-20.2	66	1	0.01	0	0.64	141.83 ± 11.10	0.1971 ± 0.0187	0.0057 ± 0.0005	36.7 ± 3.1
30.	992/MOTT2-7.1	34	0	0.01	< 1	0.08	157.59 ± 5.41	0.1107 ± 0.0075	0.0058 ± 0.0002	37.5 ± 1.3
31.	992/MOTT2-10.1	152	2	0.01	1	0.07	162.88 ± 8.34	0.1006 ± 0.0076	0.0057 ± 0.0003	36.8 ± 1.9
32.	99/2MOTT2-10.2	133	1	0.01	1	0.01	158.14 ± 3.82	0.0571 ± 0.0027	0.0062 ± 0.0002	40.1 ± 1.0
33.	992/MOTT2-9A.1	57	0	0.01	< 1	0.03	156.21 ± 6.04	0.0677 ± 0.0054	0.0062 ± 0.0002	40.1 ± 1.6
34.	992/MOTT2-5.1	37	2	0.06	< 1	0.05	162.42 ± 7.76	0.0858 ± 0.0066	0.0059 ± 0.0003	37.6 ± 1.8
35.	99/2MOTT2-5.2	187	2	0.01	1	0.01	164.91 ± 4.18	0.0553 ± 0.0034	0.0060 ± 0.0002	38.6 ± 1.0
36.	992/MOTT2-8A.1	189	2	0.01	1	0.01	159.63 ± 3.77	0.0576 ± 0.0035	0.0062 ± 0.0002	39.7 ± 1.0
37.	012/MOTT2-5.1	294	7	0.02	2	0.13	144.67 ± 3.19	0.1484 ± 0.0040	0.0060 ± 0.0001	38.7 ± 0.9
38.	*992a/MOTT2-4.1*	*43*	*1*	*0.01*	*< 1*	*0.88*	*123.27 ± 7.57*	*0.3001 ± 0.0254*	*0.0055 ± 0.0004*	*35.4 ± 2.7*
										WM: 38.5 ± 0.7
Metagabbro of Quaratta										
co-magmatic domains										
39.	QUA1-3.1	124	88	0.73	3	0.00	39.18 ± 0.94	0.0522 ± 0.0014	0.0254 ± 0.0006	161.9 ± 3.9
40.	QUA1-12.1	150	78	0.54	4	0.05	39.12 ± 0.59	0.0873 ± 0.0042	0.0243 ± 0.0004	155.0 ± 2.5
41.	QUA1-6.1	299	198	0.69	8	0.00	40.09 ± 0.62	0.0509 ± 0.0005	0.0249 ± 0.0004	158.5 ± 2.4
42.	QUA1-10.1	32	21	0.68	1	0.03	40.15 ± 2.03	0.0758 ± 0.0042	0.0241 ± 0.0012	153.3 ± 7.7
43.	QUA1-2.1	132	133	1.04	4	0.01	40.66 ± 0.71	0.0552 ± 0.0012	0.0244 ± 0.0004	155.5 ± 2.7
44.	QUA1-2.2	112	102	0.95	3	0.01	40.88 ± 0.65	0.0584 ± 0.0012	0.0242 ± 0.0004	154.0 ± 2.4
45.	QUA1-3.2	140	102	0.75	4	0.01	41.45 ± 0.72	0.0567 ± 0.0010	0.0239 ± 0.0004	152.2 ± 2.6
46.	*QUA1-6.2*	*147*	*69*	*0.48*	*3*	*0.01*	*43.30 ± 0.66*	*0.0581 ± 0.0007*	*0.0228 ± 0.0004*	*145.5 ± 2.2*
47.	*QUA1-5.1*	*26*	*12*	*0.49*	*1*	*0.04*	*42.04 ± 0.96*	*0.0799 ± 0.0040*	*0.0229 ± 0.0005*	*145.7 ± 3.4*
										WM: 155.6 ± 2.1
Misox zone–Central Alps										
Metagabbro of Hinterrhein										
co-magmatic domains										
48.	HIN1-2.1	66	49	0.77	2	0.03	39.48 ± 0.86	0.0716 ± 0.0032	0.0246 ± 0.0005	156.8 ± 3.4
49.	HIN1-10.1	58	18	0.33	1	0.04	39.66 ± 0.80	0.0785 ± 0.0069	0.0243 ± 0.0005	154.7 ± 3.4
50.	HIN1-13.1	17	2	0.13	0	0.10	34.10 ± 0.98	0.1280 ± 0.0117	0.0264 ± 0.0009	168.2 ± 5.5
51.	HIN1-11.1	272	97	0.37	7	0.01	40.13 ± 0.50	0.0556 ± 0.0011	0.0247 ± 0.0003	157.4 ± 2.0

Table 2 (Contd.)

	Sample	U (ppm)	Th (ppm)	Th/U	rad.Pb (ppm)	f_{206}	$^{238}U/^{206}Pb$ (1σ) (uncorrected)	$^{207}Pb/^{206}Pb$(1σ) (uncorrected)	$^{206}Pb/^{238}U$ (radiogenic)	Age (Ma) (1σ) $^{206}Pb/^{238}U$
52.	HIN1-14.1	332	401	1.25	10	0.01	39.02 ± 0.45	0.0549 ± 0.0010	0.0255 ± 0.0003	162.0 ± 1.9
53.	HIN1-6.1	176	71	0.42	5	0.01	37.69 ± 0.06	0.0610 ± 0.0022	0.0262 ± 0.0004	166.4 ± 2.3
54.	HIN1-9.1	216	102	0.49	6	0.01	38.44 ± 0.06	0.0607 ± 0.0014	0.0256 ± 0.0004	163.2 ± 2.5
										WM: 161.0 ± 3.9

Notes: f_{206} denotes the percentage of ^{206}Pb that is common Pb
Analyses 1–19 and 22–26 were obtained at the ANU, Canberra; all others at GSC, Ottawa
Analyses in italics were not considered for the weighted mean age calculation since they show various amounts of Pb-loss (see text for details)

University of Heidelberg. Representative analyses are listed in Table 1.

CL-imaging and study of micro-inclusions in zircon

The CL images reveal the internal structure of each sectioned-zircon grain, thus enabling the identification of regions or domains of different periods of zircon growth (e.g. cores, rims or healed fissures inside the zircon crystals). They allow one to choose best the locations for analysis and to avoid mixed age domains. In general, weak CL-emission (darker areas in the images) corresponds to high amounts of minor and trace elements, including U; strong CL-emission (lighter areas in the images) reflects low amounts of minor and trace elements (e.g. Sommerauer 1974). Thus, the U-contents can be qualitatively predicted via CL.

Inclusions of metamorphic minerals inside metamorphic zircon domains have the potential of providing information for the metamorphic conditions, under which the zircon domains formed. This information is important for the interpretation of ages obtained from metamorphic zircon domains containing inclusions. For this reason we carried out a detailed study to identify the mineral inclusions within the zircons and analysed them by electron microprobe, as described below. Caution was paid to the fact that some of them proved to be not 'real' inclusions but rather located in—healed—fissures crosscutting the zircon crystals (see below).

Flaser metagabbro at Guggilihorn, SE of Simplon

The zircons separated from this rock are quasi-equidimensional with variably resorbed outlines. Resorption features indicate the presence of abundant fluids during metamorphism. In CL, the zircons show oscillatory-zoned cores, typical for zircons crystallizing in a melt or fluid, surrounded by metamorphic rims bright in CL. The metamorphic rims are relatively narrow (e.g. Fig. 4a), less than 10 μm in width and/or have very low U-contents, and so no SHRIMP-analyses were possible. In some cases, broader metamorphic rims, richer in U are observed, however, with abundant inclusions (e.g. Fig. 4b, c), which again did not allow us to locate a SHRIMP spot in an inclusion-free area for obtaining the metamorphic age.

Electron microprobe analyses carried out on inclusions within metamorphic zircon domains revealed the presence of amphibole, chlorite and, more rarely, phengite (Table 1). Chlorites, and sometimes also amphiboles, are in many cases surrounded by minute cracks cutting through the zircon crystals, which implies that chlorite and, at least partly, also amphibole

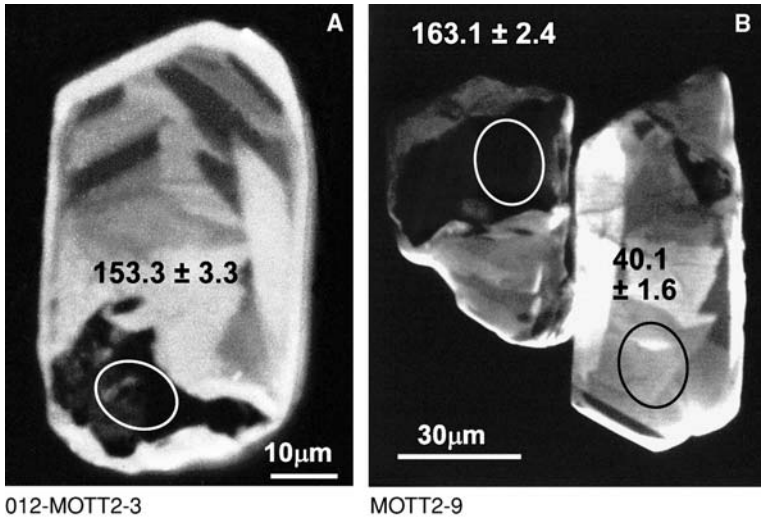

Fig. 5 CL images of zircon crystals from the amphibolitized eclogite at Passo del Mottone, Antrona ophiolites. Crystal (**a**) and left grain of (**b**) consist of dark cores (interpreted to be of magmatic origin) surrounded by a CL-bright metamorphic domain. In most zircons, the metamorphic domain constitutes the largest part of the crystal or even the entire crystal (e.g. right crystal of **b**). See text for details

formed along cracks inside the zircon crystals after the formation of the metamorphic zircon domains and so are not real inclusions. It is worth noting that these cracks can only be identified on the CL-pictures by their contrasting—brighter—CL intensity, while in SE-pictures, they are not visible (e.g. see bright CL parts crosscutting zircon in Fig. 4a; cracks are undetectable on the SE picture). Phengite inclusions were identified and analyzed in two zircon crystals (e.g., Fig. 4c, Table 1). These phengites have Si-contents of 3.45–3.47 (Si atoms per formula unit) thereby preserving a HP signature. Based on the phengite geobarometer suggested by Massonne and Schreyer (1987), these Si-values indicate pressures of ca. 13–15 kbar for metamorphism (for an assumed T range of 500–650°C). These pressures are considered as minimum pressures, since phengite does not coexist with K-feldspar and quartz, as suggested by Massonne and Schreyer (1987). The presence of Si-rich phengite inclusions in metamorphic zircon domains is also the only indication for a HP pre-history of this very strongly retrograded metagabbro from Guggilihorn, as the phengite inclusions could remain protected from the later action of fluids inside the zircon crystals.

Amphibolitized eclogite at Passo del Mottone

The zircons separated from this rock are commonly prismatic and relatively small, usually ca. 60 μm long. In CL, they show poorly preserved, dark magmatic cores surrounded by broad metamorphic rims with homogeneous, bright CL-patterns or occasionally with sector zoning (Fig. 5).

Inclusions of rutile (a couple of micrometers-large) were found in metamorphic zircon domains of this amphibolitized eclogite. The predominant Ti-phase in the rock matrix is sphene, which is very abundant, while rutile is occasionally preserved as a relic inside sphene. As is commonly the case in metabasic rocks, the HP Ti-phase is rutile, while sphene formed during the amphibolite-facies overprint. The fact that the rutile inclusions found in the metamorphic zircon domains are not altered to sphene indicates that they were enclosed in zircon before the amphibolite-facies overprint, and therefore, the age of the metamorphic zircon domains would reflect the time before the onset of amphibolitization, practically the eclogite-facies metamorphism.

Amphibolite at Quarata, S of Domodossola

The Quarata amphibolite contains relatively large zircons (commonly >150–200 μm in length), which indicates that the protolith of this rock was probably gabbro and not basalt, since such co-magmatic zircons cannot normally crystallize in the rapidly cooling basaltic melts. The zircon crystals of this rock consist exclusively of a single (magmatic) domain with weak oscillatory zoning under CL (Fig. 6). No metamorphic domains are observed, probably because the temperature was relatively low and zircon could not recrystallize (or form newly) and/or because the amount of fluids during metamorphism was limited (see above under Sect. 3.1).

Metagabbro at Hinterrhein (Misox zone)—Central Alps

The metagabbro of Hinterrhein contains zircons consisting exclusively of magmatic domains with distinct oscillatory zoning (Fig. 7). Some zircon crystals show faint oscillatory zoning at the outermost parts (Fig. 7, both crystals), probably because of trace element leaching, due to the action of fluids (compare e.g., Gebauer 1996, his Fig. 15). It is worth noting that such crystal domains show the same age as the ones with strong oscillatory zoning. This implies that leaching of trace elements must have taken place shortly after crystal growth in an environment rich in fluids. No metamorphic rims were observed in these zircons, obviously due to the relatively low temperature of metamorphism and/or limited amounts of fluids.

SHRIMP results and interpretation

Flaser metagabbro at Guggilihorn, SE of Simplon

We have analyzed 13 spots from the magmatic zircon domains of this metagabbro. Two analyses (nr. 11 and 13 of Table 2) overlap two neighboring domains (magmatic and metamorphic), as indicated by post-SHRIMP CL-studies, and therefore, yield mixed ages. One analysis (nr. 12) shows minor radiogenic Pb-loss, possibly due to subsequent metamorphism(s). On a TW diagram (Fig. 8), ten analyses plot on a mixing line between common Pb and a radiogenic $^{238}U/^{206}Pb$ end member. The weighted mean of the radiogenic $^{206}Pb/^{238}U$ ages for these 10 analyses gives 155.2 ± 1.6 Ma (MSWD = 1.2; error at the 95% c.l.). This age is interpreted as the time of crystallization of the gabbroic protolith.

As mentioned above, it was not possible to date the metamorphic rims of the zircons from the metagabbro of Guggilihorn. However, an attempt to determine a general estimate about the time of metamorphism yielded the following dates: 75.1 ± 4.4 Ma, 68.5 ± 2.2 Ma, 61.0 ± 2.2 Ma and 54.2 ± 4.9 Ma (1σ error). For these analyses, the SHRIMP-spots were located partly (ca. 15%) on the neighboring older core domain (analyses 15 and 16 the latter located in addition on inclusions), or in metamorphic domains with inclusions (analyses 17 and 18). The youngest date (54.2 ± 4.9 Ma; 1σ error) may be considered as providing a maximum estimate for the time of metamorphism.

Amphibolitized eclogite at Passo del Mottone

Eleven analyses were obtained from the metamorphic rims of this rock. On a Tera–Wasserburg diagram

(Fig. 9a), they plot on a mixing line between common Pb and the radiogenic $^{238}U/^{206}Pb$ end member, with a weighted mean $^{206}Pb/^{238}U$ age of 38.5 ± 0.7 Ma (MSWD = 0.98; error at the 95% c.l.). We interpret this age as reflecting the time of the high-P, eclogite-facies metamorphism. This interpretation is based on: (1) the general empirical observation of numerous CL-controlled ion microprobe studies of complex (poly)metamorphic zircons from orogens worldwide, combined with the petrology of the rocks and REE analyses of metamorphic zircon domains (see e.g. Liati and Gebauer 2003 and references therein or Rubatto et al. 2003 for this issue). It was repeatedly ascertained that zircon responds to metamorphic recrystallization only at or above T conditions corresponding to the upper amphibolite-/granulite- or high-temperature eclogite-facies (e.g., Vavra et al. 1999 and references therein), unless unusually high amounts of fluids are present, in which case recrystallization may take place at lower *T*. Thus, the age obtained from the metamorphic domains of the zircon most probably reflects the time when the rocks were at or close to the metamorphic peak. Since the rates of exhumation are usually high (> 1–2 cm/year), as identified in several (ultra) high-pressure [(U)HP] rocks from orogens worldwide (e.g., Gebauer et al. 1997; Amato et al. 1999; Liati and Gebauer 1999; Cartwright and Barnicoat 2002 and references therein) the metamorphic peak refers roughly to both *T* and *P*. The relatively short time difference between *T* peak and *P* peak is commonly unresolvable within the uncertainty of the current geochronological technique. Therefore, the age data obtained from metamorphically recrystallized zircon crystals (or crystal domains) of (U)HP rocks correspond to time of peak metamorphism, with respect to both *P* and *T*. (2) In this particular case of the amphibolitized eclogite of Mottone, the presence of rutile inclusions in metamorphic zircon domains (in contrast to rutile in the matrix, which is altered to sphene) confirms this general observation (see also Sect. 5.2). Therefore, the 38.5 ± 0.7 Ma age obtained from the metamorphic domains of zircons is a good approximation for the time of HP metamorphism.

Dating the magmatic zircon cores from the amphibolitized eclogite at Passo del Mottone was complicated by the fact that these cores are either not present (completely consumed during metamorphic recrystalli-

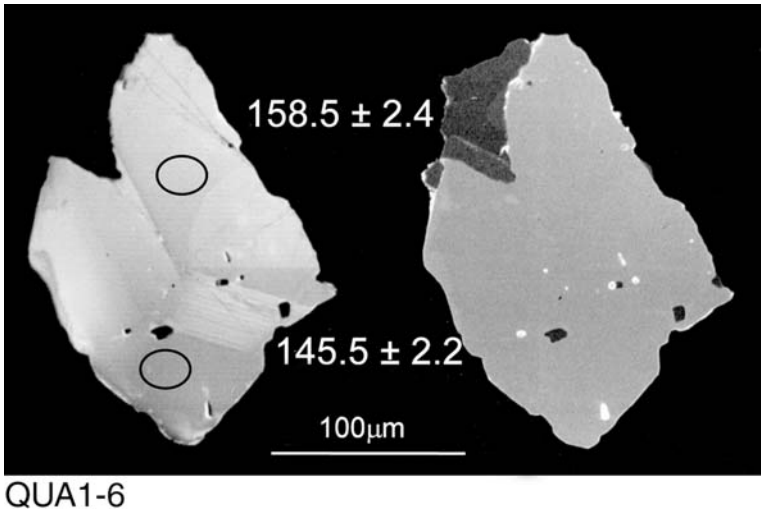

Fig. 6 CL (*left part* of picture) and SE (*right part* of picture) images of a zircon crystal from the amphibolite of Quarata, Antrona ophiolites, consisting exclusively of a single domain of magmatic origin with weak oscillatory zoning

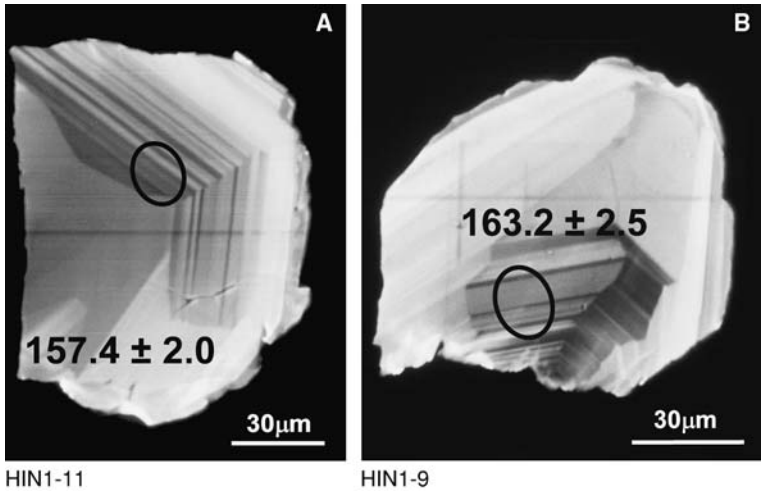

Fig. 7 CL images of zircon crystals from the metagabbro of Hinterrhein, Misox zone, consisting entirely of a magmatic domain. Oscillatory zoning is quite well expressed, except for the outer part of the crystals where leaching of trace elements took place, probably immediately after crystal growth in a fluid-rich environment (see also text)

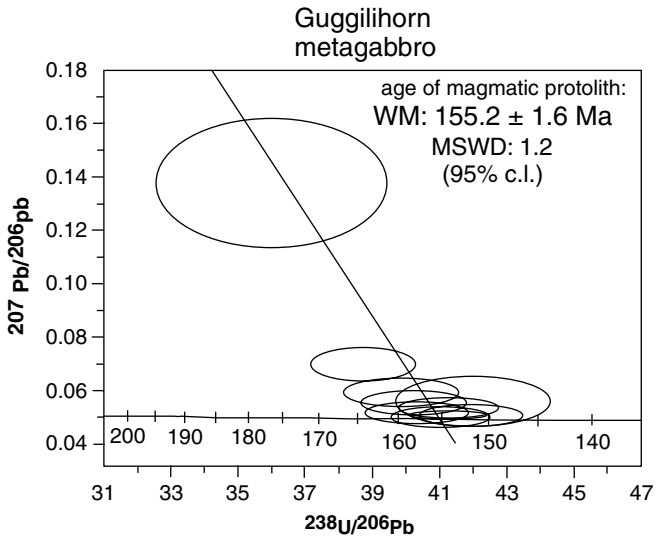

Fig. 8 Tera–Wasserburg diagram with data of zircons from the metagabbro of Guggilihorn, Antrona ophiolites. Ten analyses from the co-magmatic, oscillatory zoned zircon domains plot on a mixing line with common Pb and radiogenic $^{238}U/^{206}Pb$ as end members, intersecting the concordia curve at 155.2 ± 1.6 Ma, interpreted as the time of crystallization of the gabbroic protolith

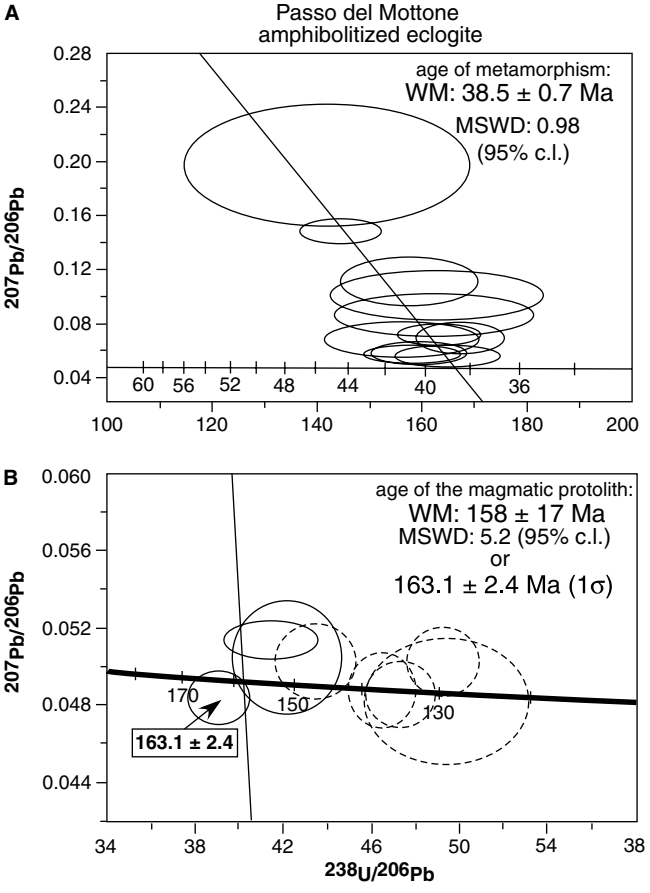

Fig. 9 Tera–Wasserburg diagrams with data of zircons from the amphibolitized eclogite of Passo del Mottone, Antrona ophiolites. In (**a**), eleven analyses from the metamorphic zircon domains plot on a mixing line with common Pb and radiogenic $^{238}U/^{206}Pb$ as end members, and yield a weighted mean $^{206}Pb/^{238}U$ age of 38.5 ± 0.7 Ma. In (**b**), three analyses from the co-magmatic zircon cores plot on a mixing line intersecting the concordia curve at 158 ± 17 Ma. Another five analyses plot to the right side of the mixing line (*dashed ellipses*), due to Pb-loss. Alternatively, the analysis, which yields the highest age (163.1 ± 2.4 Ma, 1σ: *leftmost ellipse on the diagram*) can be considered as closest to the protolith age; in this case the two analyses represented by the ellipses touching the mixing line (20 and 21 of Table 2) would be interpreted also as showing minor Pb-loss

zation) or preserved only as small relictic domains and then only in a few zircon crystals (e.g., Fig. 5). It was therefore difficult to fit a 10 μm diameter SHRIMP-spot entirely in the core domain. As shown by post-SHRIMP CL-studies, during most of our attempts to determine a protolith age, we could not avoid overlapping and analyzing, to a smaller or larger extent, the younger neighboring metamorphic rim domain of the zircon. The dates obtained for such slightly mixed domains deviate from the real age of the magmatic cores, as they include a young component from the neighboring metamorphic domain. A few analyzed SHRIMP-spots were entirely located within the magmatic cores and yielded dates ranging between 163.1 ± 2.4 Ma and 129.3 ± 4.0 Ma (1σ errors). On a Tera–Wasserburg diagram (Fig. 9b) three of these analyses (Nr. 19, 20 and 21 in Table 2) form a coherent grouping and plot on a mixing line with common Pb and radiogenic $^{238}U/^{206}Pb$ as end members and yield a weighted mean age of 158 ± 17 Ma (MSWD = 5.2, error at the 95% c.l.). The large error of the above weighted mean age relies on the very high student-*t* factor (= 4.3), which is due to the small number of analyses (3). The calculated ca. 158 Ma age may provide an estimate for the age of the protolith. Although the three analyses considered above for the weighted mean age calculation fit statistically on a single mixing line, it is possible that the two younger dates (nr. 20 and 21) show minor radiogenic Pb-loss (as is the case for analyses 22–26 plotting to the right of the mixing line). Based on this assumption, we could alternatively consider the oldest of these dates (163.1 ± 2.4 Ma) as a more realistic approach for the age of the protolith. It is noted that previously reported preliminary data for the eclogite of Mottone, showing a cluster of "ages" around 133 Ma were provisionally attributed to the crystallization time of the protolith of this eclogite (Liati and Gebauer 2001). However, in view of the additional analyses included in the present study, the scattering of "ages" concentrated around ca. 133 Ma are re-interpreted here rather as reflecting Pb-loss.

Amphibolite at Quarata, S of Domodossola

Seven analyses on the magmatic domains of this amphibolite yielded a weighted mean (crystallization) $^{206}Pb/^{238}U$ age at 155.6 ± 2.1 Ma (Fig. 10). This is identical—within uncertainty—to the 155.2 ± 1.6 Ma crystallization age of the Simplon metagabbro at Guggilihorn.

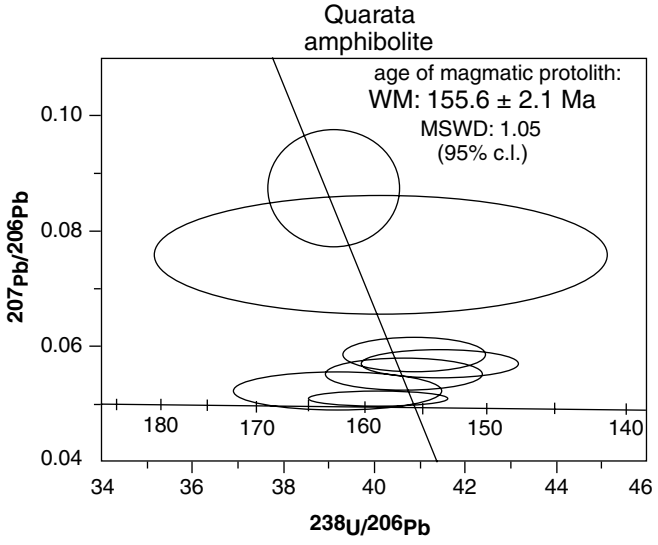

Fig. 10 Tera–Wasserburg diagram with data of zircons from the amphibolite of Quarata, Antrona ophiolites. Seven analyses from the magmatic zircon domains plot on a mixing line with common Pb and radiogenic $^{238}U/^{206}Pb$ as end members, and yield a weighted mean $^{206}Pb/^{238}U$ age of 155.6 ± 2.1 Ma, interpreted as the time of crystallization of the magmatic (gabbroic) protolith.

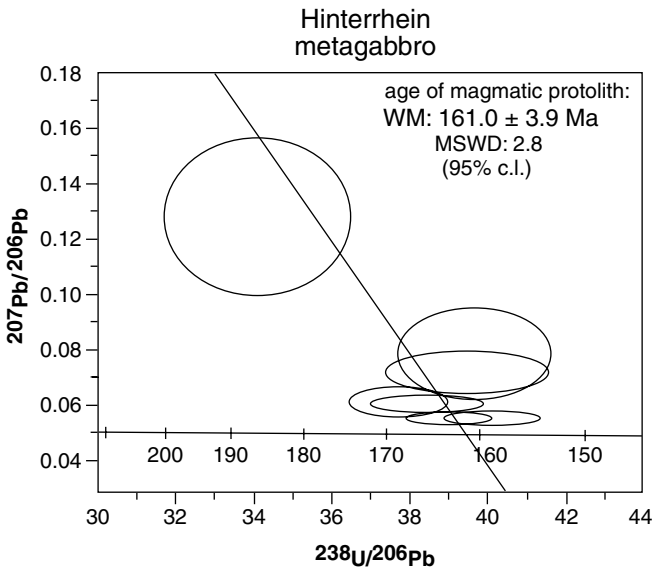

Fig. 11 Tera–Wasserburg diagram with data of zircons from the metagabbro of Hinterrhein, Misox zone. Seven analyses from the magmatic zircon domains plot on a mixing line with common Pb and radiogenic $^{238}U/^{206}Pb$ as end members, and yield a weighted mean $^{206}Pb/^{238}U$ age of 161.0 ± 3.9 Ma, interpreted as the time of crystallization of the magmatic (gabbroic) protolith

Metagabbro at Hinterrhein (Misox zone)—Central Alps

Seven analyses of the magmatic domains of this metagabbro yielded a weighted mean (crystallization) $^{206}Pb/^{238}U$ age at 161.0 ± 3.9 Ma (Fig. 11), identical—within the 95% c.l. uncertainty—to the 155.6 ± 2.1 Ma and 163.1 ± 4.8 Ma crystallization ages of the amphibolite at Quarata and the eclogite at Mottone, respectively and almost identical (with an age difference of only 0.3 Ma) to the 155.2 ± 1.6 Ma crystallization age of the Simplon metagabbro at Guggilihorn (Western Alps).

Geodynamic implications and discussion

The identification of 155.2 ± 1.6 Ma, 163.1 ± 4.8 Ma (or 158 ± 17 Ma) and 155.6 ± 2.1 Ma ages for the crystallization of three metabasites and of a 38.5 ± 0.7 Ma age for HP metamorphism of an amphibolitized eclogite from the Antrona ophiolites (Western Alps), as well as the 161.0 ± 3.9 Ma crystallization age of a metabasite of the Misox zone (Valais domain, Central Alps) raises an important issue regarding the paleogeographic reconstruction and the geodynamic evolution of the Alpine orogen. As mentioned in the 'Introduction', two oceans existed in the area of the Alps before the onset of convergence in ca. Middle/Upper Cretaceous times: the PL ocean, as the principal ocean, which opened from the Middle Jurassic onwards, and the Valais ocean which opened later (from the Late Jurassic to Early Cretaceous). Geochronological data available so far on the relatively small exhumed part of PL oceanic crust suggest crystallization ages between 148 ± 3 Ma and 166 ± 1 Ma (see summary by Liati et al. 2003 and references therein), in agreement with paleontological data (e.g. De Wever and Baumgartner 1995). The time of opening of the Valais ocean is based on paleontological data (e.g. Frisch 1979; Trümpy 1980; Florineth and Froitzheim 1994; Stampfli et al. 1998), while geochronological data are reported only for oceanic rocks forming during the late stages of opening (at ca. 93 Ma; Liati et al. 2003).

Based on the geochronological and paleontological data for the two Alpine oceans, the ca. 155 Ma and the 163.1 ± 4.8 Ma protolith ages obtained for the metabasites of the Antrona ophiolites (Guggilihorn, Quarata and Mottone) are within the time span accepted for the formation of Piemont–Ligurian oceanic crust. The metabasite sample of the Misox zone (area of Hinterrhein, Central Alps), which geotectonically clearly belongs to the Valais domain (e.g. Schmid et al. 1996), also yielded a crystallization age of 161.0 ± 3.9 Ma. This age does not fall into the age range expected for the Valaisan geotectonic unit of Misox. Instead, it clearly falls into the range of ages reported for Piemont–Ligurian oceanic crust. Based on this 161.0 ± 3.9 Ma, PL crystallization age and taking into consideration structural geological data which attribute the Misox zone to the Valais domain, we infer that PL crust was placed partly within a Valaisan structural position. This hypothesis is confirmed by the age of metamorphism obtained from the amphibolitized eclogite of Passo del Mottone (38.5 ± 0.7 Ma). This age corresponds to the time of metamorphism reported for rocks of the Valais domain

in other areas of the Central and Western Alps: metamorphic ages of 37.1 ± 0.9 Ma (Chiavenna ophiolites, Central Alps; Liati et al. 2003) and 40.4 ± 0.7 Ma (Balma unit, Western Alps; Liati et al. 2002; see also Fig. 2b). In contrast to these metamorphic ages reported for the Valais domain, subduction and (U)HP metamorphism in the PL ocean has taken place at ca. 44–45 Ma (zircon SHRIMP-data by Rubatto et al. 1998 and Rubatto and Hermann 2003) or between 48.8 ± 2.1 and 40.6 ± 2.6 Ma. The latter age range (not fully consistent with the SHRIMP-data) was interpreted by Lapen et al. (2003) to reflect the duration of the prograde PT path, based on their Lu-Hf data, as well as on Sm-Nd data by Amato et al. (1999).

In the present case of metabasic rocks from the Antrona ophiolites and the Misox zone, we are therefore confronted with an apparent paradox: metabasic rocks in a Valaisan structural position (undisputed for the Misox zone and controversial in the case of the Antrona ophiolites) yield a protolith age typical for PL oceanic crust but a metamorphic age characterizing Valaisan metamorphic rocks (ca. 6 Ma younger than metamorphism of PL rocks). This paradox can be resolved if PL oceanic crust was partly positioned within the Valais domain. Paleogeographic reconstruction models involving re-rifting of PL oceanic crust during the Cretaceous opening of the Valais ocean was already suggested by Stampfli (1993). The geochronological data obtained in the present study support this scenario. We assume that the Valais ocean opened during the Early Cretaceous along a trace cutting obliquely across the northwestern margin of the PL ocean (Fig. 12). The new ocean thus separated the eastward-narrowing Ibero-Briançonnais from Europe. Where the trace of the Valais ocean entered the PL ocean, Valais opening implied re-rifting of PL oceanic lithosphere. Towards east, the Valais spreading center merged into the mid-ocean ridge of the Piemont–Ligurian ocean, which had already been active since the Middle Jurassic. Towards west, we assume that the Valais ocean was connected with the tip of the northward-propagating Atlantic through the Bay of Biscay and the Pyrenean rift or ocean (Frisch 1979; Stampfli 1993). The reason for the obliquity of the Valaisan rift with respect to the northwestern margin of the PL ocean is the reorganisation of plate kinematics caused by the northward propagation of the Atlantic. In the course of the Cretaceous, the tip of the Briançonnais moved east relative to Europe (Fig. 12b and Stampfli 1993). Opening of the Valais basin lasted at least until 93 Ma (age of the metagabbro in the Chiavenna ophiolite, Liati et al. 2003) before convergence between Briançonnais and Europe started. The opening and sinistral motion together led to the situation depicted in Fig. 12b. An area of Jurassic ocean floor, originally formed in the PL basin, was captured in the Valais basin (upper left part of 'Jurassic ocean floor' in Fig. 12b). We assume that the Jurassic gabbros from the Antrona and Misox zones represent this area.

According to this hypothesis, the age distribution in the Valais basin is asymmetric: on the southeastern side of the basin, Briançonnais continental crust is directly adjacent to Cretaceous ocean floor, as observed in the Tasna nappe of the Engadine window (Florineth and Froitzheim, 1994), whereas in the northern part, Jurassic ocean floor faces the European continental crust along a passive margin that originally formed in the PL ocean (Stampfli 1993) (see also Fig. 13b). When the Briançonnais and Europe converged during the Early Tertiary, parts of oceanic crust of both PL and Valaisan origin were subducted together at ca. 39 Ma, that is ca. 6 Ma later than the PL geotectonic domain located south of the Briançonnais.

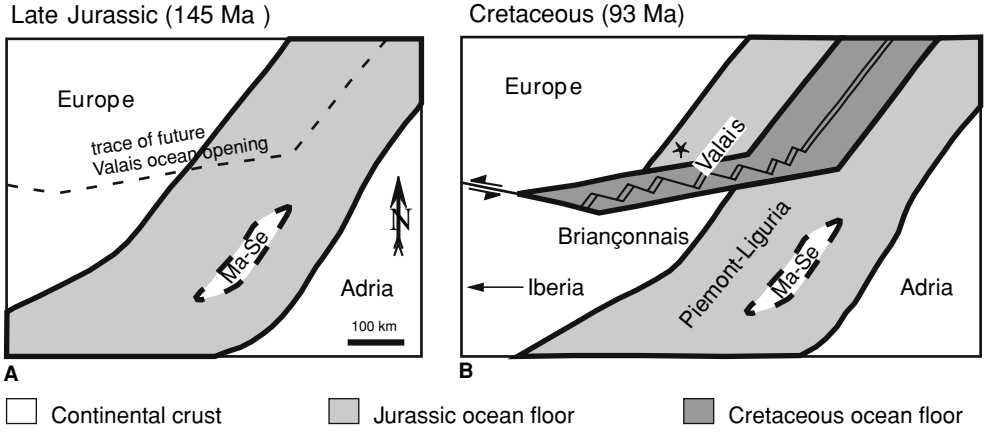

Fig. 12 Schematic paleogeographic scenario explaining the occurrence of PL ocean floor within the Valais geotectonic domain. In (**a**), Late Jurassic ocean floor forms as part of the PL ocean. In (**b**), younger Valaisan oceanic crust forms due to oblique opening (partly re-rifting within existing PL oceanic crust), thus incorporating the older PL oceanic crust to the N of the newly formed Briançonnais peninsula, within the Valais domain (see also text). The star indicates the paleogeographic position of the Antrona ophiolites and of the Misox metagabbro dated in the present study, based on the above scenario. The "island" within the Piemont–Ligurian ocean (Ma-Se) is the Margna-Sesia continental fragment. It is outlined with a dashed line indicating that the positioning of this continental fragment within the PL ocean, as well as its extent are speculative

Regarding the question of the origin of the Antrona ophiolites (Fig. 3), our new data support a paleogeography where Antrona was geometrically part of the Valais basin, between the Briançonnais and Europe (Fig. 13). The protolith ages would also allow to place Antrona southeast of the Briançonnais but the metamorphic age (38.5 ± 0.7 Ma) strongly argues in favor of a position northwest of the Briançonnais.

Apart from this, the re-rifting model predicts that east of the tip of the Briançonnais (which is probably located in the Engadine window, Froitzheim et al. 1996), Cretaceous ocean formed within the Jurassic PL ocean (Fig. 12b). In fact, radiolarite, the typical sediment of the PL ocean's margins, occurs both in the Ultrahelvetic sequence of eastern Austria, that is, on the distal European continental margin (Tollmann 1985, p 332), and in the Lower Austroalpine nappes in the frame of the Tauern window, that is, on the distal Adriatic margin (Tollmann 1977). Therefore, the Cretaceous ocean floor in the Eastern Alps, if it was present, was bordered by Jurassic ocean floor on both sides. Remnants of such Cretaceous ocean floor may exist in the Glockner nappe of the Tauern window, but unfortunately, ophiolites from this unit have not yet been dated.

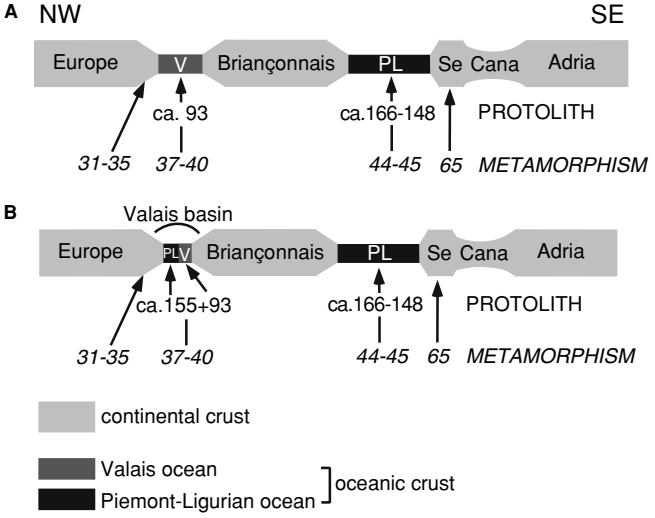

Fig. 13 Schematic profiles from the European to the Adriatic plate (NW to SE) representing a model for the paleogeographic situation in the area of the Central and Western Alps (based on Gebauer 1999). Both (**a**) and (**b**) are based on a series of radiometric data (mainly SHRIMP) for both protolith and metamorphic ages. The difference in profile (**b**) compared to (**a**) is that it represents the situation suggested for Misox and Antrona, where PL oceanic lithosphere is partly positioned inside the Valais domain. Radiometric data are as follows: for the European margin they include Alpe Arami (Gebauer 1996), Dora Maira (Gebauer et al. 1997) and Monte Rosa (Gornergrat; Rubatto and Gebauer 1999); for the Valais basin they include the ophiolites of Valais origin in Chiavenna unit, Central Alps (Liati et al. 2003) and Balma unit, south of the Monte Rosa nappe, Western Alps (e.g., Liati et al. 2002). For the Piemont–Ligurian ocean, see Liati et al. (2003 and references therein); for the Sesia zone data are from Rubatto et al. (1999). V: Valais; PL: Piemont–Ligurian; Se: Sesia; Cana: Canavese

During the many years of geological research in the Alps, different models were proposed for their paleogeographic evolution, referring to the time prior to the onset of the Alpine orogeny (e.g. review by Escher et al. 1997; Froitzheim 2001 and references therein). Based on a series of geochronological data, mainly SHRIMP, obtained over the last ca. 10 years in metamorphic rocks of the Alps, a model involving successive subduction/collision episodes starting at ca. 65 Ma in the SSE (Sesia zone) and getting younger to the NNW, through Piemont–Ligurian metamorphic rocks (at ca. 44–45 Ma), metamorphic rocks of the Valais ocean (at 40–37 Ma) to the European margin (35–31 Ma) was suggested (Fig. 13a; see e.g. summary by Gebauer 1999 and references therein). Based on the new geochronological data obtained in this paper, the scheme shown in Fig. 13a can be slightly modified, as shown in Fig. 13b, in that part of the PL oceanic crust was possibly positioned in the geotectonic domain occupied by the Valais basin.

Re-rifting of oceanic crust as proposed in the present article was also described from other places, e.g., Oman (Marquer et al. 1998). It leads to specific sedimentary, tectonic, metamorphic, and magmatic processes. To look for the signature of these processes, especially in the Penninic units of the Eastern Alps, would be an interesting task for future work.

Acknowledgments We appreciate very much the help of M. Hamilton, R. Stern, N. Rayner and W. Davis during various stages of the SHRIMP work at the Geological Survey of Canada, Ottawa. D. Gebauer, ETH Zurich, contributed substantially with discussions and remarks on an early draft of the manuscript. Many thanks also to P. Meyer, Heidelberg, for his help with the microprobe analyses. We acknowledge the constructive review by K. Mezger, Münster, and R. Oberhänsli, Potsdam. Many thanks also to W. Schreyer, Bochum, for the editorial support. This study was supported by a grant of the Swiss National Science Foundation (20-63767.00). The work of NF was supported by the "Deutsche Forschungsgemeinschaft", grant Nr. FR700/6.

References

Amato JM, Johnson CM, Baumgartner LP, Beard BL (1999) Rapid exhumation of the Zermatt-Saas ophiolite deduced from high-precision Sm-Nd and Rb-Sr geochronology. Earth Planet Sci Lett 171:425–438

Cartwright I, Barnicoat, AC (2002) Petrology, geochronology and tectonics of shear zones in the Zermatt-Saas and Combin zones of the Western Alps. Jour Metam Geol 20:263–281

Colombi A (1989) Metamorphisme et geochimie des roches mafiques des Alpes ouest-centrales (geoprofil Viege-Domodossola-Locarno). Mémoires de Géologie, Lausanne 4:216

Colombi A, Pfeifer HR (1986) Ferrogabbroic and basaltic metaeclogites from the Antrona mafic-ultramafic complex and the Centovalli-Locarno region (Italy and southern Switzerland)-First results. Schweiz Mineral Petrogr Mitt 66:99–110

Compston W, Williams IS, Kirschvink JL, Zichao Z, Guogan M (1992) Zircon U-Pb ages for the Early Cambrian time-scale. Jour Geol Soc London 149:171–184

Cumming GL, Richards GR (1975) Ore lead isotope ratios in a continuously changing Earth. Earth Planet Sci Lett 28:155–171

De Wever P, Baumgartner PO (1995) Radiolarians from the base of the Supra-ophiolitic Schistes Lustrés formation in the Alps (Saint-Véran, France and Traversiera Massif, Italy). In: Baumgartner PO, ÓDogerthy L, Gorican S, Urquhart E, Pillevuit A, De Wever P (eds) Middle Jurassic to Lower Cretaceous Radiolaria of Tethys: occurrences, systematics, biochronology. Mém Géol (Lausanne) 23:725-730

Escher A, Hunziker J-C, Marthaler M, Masson H, Sartori M, Steck A (1997) A Geologic framework and structural evolution of the western Swiss-Italian Alps. In: Pfiffner OA, Lehner P, Heitzmann PZ, Mueler S, Steck A (eds) Deep structure of the Swiss Alps: results of NRP 20. Birkhäuser, Basel, pp 205–221

Florineth D, Froitzheim N (1994) Transition from continental to oceanic basement in the Tasna nappe (Engadine window, Graubünden, Switzerland): evidence for Early Cretaceous opening of the Valais ocean. Schweiz Mineral Petrogr Mitt 74:134–137

Frey M, Ferreiro-Mählmann R (1999) Alpine metamorphism of the Central Alps. Schweiz Mineral Petrogr Mitt 79:135–154

Frisch W (1979) Tectonic progradation and plate tectonic evolution of the Alps. Tectonophysics 60:121–139

Froitzheim N (2001) Origin of the Monte Rosa nappe in the Pennine Alps—a new working hypothesis. Geol Soc Amer Bull 113:604-614

Froitzheim N, Schmid SM, Frey M (1996) Mesozoic paleogeography and the timing of eclogite-facies metamorphism in the Alps: a working hypothesis. Eclogae geol Helv 89:81–110

Gansser A (1937) Der Nordrand der Tambodecke. Schweiz Mineral Petrogr Mitt 17:291–522

Gebauer D (1996) A P-T-t path for an (ultra?-) high-pressure ultramafic/mafic rock association and its country rocks based on SHRIMP-dating of magmatic and metamorphic zircon domains. Example: Alpe Arami (Central Swiss Alps) In: Earth processes: reading the isotopic code. Geophys Monogr 95:107–111

Gebauer D (1999) Alpine geochronology of the Central and Western Alps: new constraints for a complex geodynamic evolution. Schweiz Mineral Petrogr Mitt 79:191–208

Gebauer D, Schertl H-P, Brix M, Schreyer W (1997) 35 Ma old ultrahigh-pressure metamorphism and evidence for very rapid exhumation in the Dora Maira Massif, Western Alps. Lithos 41:35–24

Heinrich CA (1983) Die regionale Hochdruckmetamorphose der Aduladecke, Zentralalpen, Schweiz. Dissertation, ETH Nr 7282, 213 pp

Hellman PL, Green TH (1979) The role of sphene as an accessory phase in the high-pressure partial melting of hydrous mafic compositions. Earth Planet Sci Lett 42:191–201

Jäger E (1973) Die Alpine Orogenese im Lichte der radiometrischen Altersbestimmung. Eclogae Geol Helv 66:11–21

Keller LM, Schmid SM (2001) On the kinematics of shearing near the top of the Monte Rosa nappe and the nature of the Furgg zone in Val Loranco (Antrona valley, N Italy): tectono-metamorphic and paleogeographical consequences. Schweiz Mineral Petrogr Mitt 81:347–367

Lapen TJ, Johnson CM, Baumgartner LP, Mahlen NJ, Beard BL, Amato JM (2003) Burial rates during prograde metamorphism of an ultra-high-pressure terrane: an example from Lago di Cignana, western Alps, Italy. Earth Planet Sci Lett 215:57–72

Liati A, Gebauer D (1999) Constraining the prograde and retrograde P-T-t path of Eocene HP-rocks by SHRIMP dating of different zircon domains: inferred rates of heating, burial, cooling and exhumation for central Rhodope, northern Greece. Contrib Mineral Petrol 135:340–354

Liati A, Gebauer D (2001) U-Pb SHRIMP-dating of zircon domains from eclogites of Antrona (Western Alps): evidence for a Valais ocean origin. EUG 11, Journal of Conference Abstracts 6:600

Liati A, Gebauer D (2003) Geochronological constraints for the time of metamorphism in the Gruf Complex (Central Alps) and implications for the Adula-Cima Lunga nappe system. Schweiz Minetral Petrogr Mitt 83:159–172

Liati A, Gebauer D, Froitzheim N (2002) Late Cretaceous basic oceanic magmatism in the Valais ocean, Western and Central Alps: geochronological evidence and paleogeographic implications. Annual Meeting of the Swiss Academy of Natural Sciences, Davos, Abstract volume, p 26

Liati A, Gebauer D, Fanning CM (2003) The youngest basic oceanic magmatism in the Alps (Late Cretaceous; Chiavenna unit; Central Alps): geochronological constraints and geodynamic significance. Contrib Mineral Petrol 146:144–158

Ludwig K (2000) User's Manual for Isoplot/Ex, version 2.4. A geochronological Toolkit for Microsoft Excel. Berkeley Geochronological Center, Special Publication No. 1a, 53 pp

Marquer D, Mercolli I, Peters T (1998) Early Cretaceous intra-oceanic rifting in the Proto-Indian Ocean recorded in the Masirah Ophiolite, Sultanate of Oman. Tectonophysics 292:1–16

Massonne HJ, Schreyer W (1987) Phengite geobarometry based on the limiting assemblage with K-feldspar, phlogopite and quartz. Contrib Mineral Petrol 96: 212–224

Oberhänsli R (1986) Blue amphiboles in metamorphosed Mesozoic mafic rocks from the Central Alps. Geol Soc Amer Memoir 164:239–247

Oberhänsli R (1994) Subducted and obducted ophiolites of the Central Alps: Paleotectonic implications deduced by their distribution and metamorphic overprint. Lithos 33:109–118

Paces JB, Miller JD (1993) Precise U-Pb ages of Duluth Complex and related mafic intrusions, northeastern Minnesota: Geochronological insights to physical, petrogenetic, paleomagnetic, and tectonomagmatic process associated with the 1.1 Ga Midcontinent Rift System. J Geophys Res 98:13997–14013

Pfeiffer HR, Colombi A, Ganguin J (1989) Zermatt-Saas and Antrona zone: a petrographic and geochemical comparison of polyphase metamorphic ophiolites of the West-Central Alps. Schweiz Mineral Petrogr Mitt 69:217–236

Platt JP (1986) Dynamics of orogenic wedges and the uplift of high-pressure metamorphic rocks. Geol Soc Am Bull 97:1037–1053

Pleuger J, Hundenborn R, Kremer K, Babinka S, Kurz W, Jansen E, Froitzheim N (2003) Structural evolution of Adula nappe, Misox zone, and Tambo nappe in the San Bernardino area: Constraints for the exhumation of the Adula eclogites. Mitt Österr Geol Ges 94:99–122

Ring U (1992) The Alpine geodynamic evolution of Penninic nappes in the eastern Central Alps: geothermobarometric and kinematic data. J Metamorphic Geol 10:33–53

Rubatto D, Gebauer D (1999) Eo/Oligocene (35 Ma) high-pressure metamorphism in the Gornergrat Zone (Monte Rosa, Western Alps): implications for paleogeography. Schweiz Mineral Petrogr Mitt 79:353–362

Rubatto D, Hermann J (2003) Zircon formation during fluid circulation in eclogites (Monviso, Western Alps): implication for Zr and Hf budget in subduction zones. Geochim Cosmochim Acta 67:2173–2187

Rubatto D, Gebauer D, Fanning M (1998) Jurassic formation and Eocene subduction of the Zermatt-Saas Fee ophiolites: implications for the geodynamic evolution of the Central and Western Alps. Contrib Mineral Petrol 132:269–287

Rubatto D, Liati A, Gebauer D (2003) Dating UHP metamorphism. EMU Note Mineral 5:341–363

Schmid SM, Pfiffner OA, Froitzheim N, Schönborn G, Kissling E (1996) Geophysical-geological transect and tectonic evolution of the Swiss-Italian Alps. Tectonics 15:1036–1064

Sommerauer J (1974) Trace elements distribution patterns and mineralogical stability of zircons—an application for combined electron microprobe techniques. Electron Microsc Soc Southern Africa, Proc 4:71–72

Stampfli GM (1993) Le Briançonnais, terrain exotique dans les Alpes?. Eclogae Geol Helv 86:1–45

Stampfli GM, Mosar J, Marquer D, Marchant R, Baudin T, Borel G (1998) Subduction and obduction processes in the Swiss Alps. Tectonophysics 296:159–204

Steck A, Epard J-L, Escher A, Gouffon Y, Masson H (2001) Carte tectonique des Alpes de Suisse occidentale et des régions avoisinantes, 1:100,000, Notice explicative. Office fédéral des eaux et de la géologie. Bern, Switzerland, p 73

Stern R (1997) The GSC Sensitive High Resolution Ion Microprobe (SHRIMP): analytical techniques of zircon U-Th-Pb age determinations and performance evaluation. In: Radiogenic Age and isotope studies: Report 10; Geological Survey of Canada, Current research, p 1–31

Stern RA, Amelin Y (2003) Assessment of errors in SIMS zircon U-Pb geochronology using a natural zircon standard and NIST SRM 610 glass. Chem Geol 197:111–142

Tera F, Wasserburg GJ (1972) U-Th-Pb systematics in three Apollo 14 basalts and the problem of initial Pb in lunar rocks. Earth Planet Sci Lett 14:281–304

Tollmann A (1977) Geologie von Österreich—Band 1. Deuticke, Vienna, 766 pp

Tollmann A (1985) Geologie von Österreich—Band 2. Deuticke, Vienna, 710 pp

Trommsdorff, V (1966) Progressive Metamorphose kieseliger Karbonatgesteine in den Zentralalpen zwischen Bernina und Simplon. Schweiz Mineral Petrogr Mitt 46:431–460

Trümpy R (1980) Geology of Switzerland, a guide book Part A: An outline of the geology of Switzerland. Scweiz Geol Komm, Wepf and Co, Basel, 104 pp

Vavra G, Schmid R, Gebauer D (1999) Internal morphology, habit and U-Th-Pb microanalysis of amphibolite-to-granulite facies zircons: geochronology of the Ivrea Zone (Southern Alps). Contrib Mineral Petrol 134:380–404

Wenk E (1956) Die lepontinische Gneissregion und die jungen Granite der Valle della Mera. Eclogae geol Helv 49:251–265

Williams IS (1998) U-Th-Pb Geochronology by Ion Microprobe. In: McKibben MA, Shanks III WC and Ridley WI (eds): Applications of microanalytical techniques to understanding mineralizing processes. Reviews in Economic Geology 7:1–35